

PAPER • OPEN ACCESS

Effect of Calcining Time on the Room Temperature Ionic Conductivity of W, Y and Al Co-doped $\text{Li}_7\text{La}_3\text{Zr}_2\text{O}_{12}$ Solid Electrolyte

To cite this article: Xiaozhou Liu *et al* 2019 *IOP Conf. Ser.: Earth Environ. Sci.* **267** 062041

View the [article online](#) for updates and enhancements.

Effect of Calcining Time on the Room Temperature Ionic Conductivity of W, Y and Al Co-doped $\text{Li}_7\text{La}_3\text{Zr}_2\text{O}_{12}$ Solid Electrolyte

Xiaozhou Liu¹, Xiaozhen Liu^{2,*}, Xingjue Shi² and Jie Chen³

¹Gannan Normal University, Jiangxi, 341000, China

²School of Chemical and Environmental Engineering, Shanghai Institute of Technology, Shanghai, 201418, China

³Regenia AB, Stockholm, 10691, Sweden

*Corresponding author's e-mail: liuxiaozhen5291@163.com

Abstract. $\text{Li}_{5.76}\text{La}_3\text{Zr}_{1.59}\text{W}_{0.35}\text{Y}_{0.06}\text{Al}_{0.2}\text{O}_{12}$ (W, Y, Al-LLZO) solid electrolyte was prepared using the solid-state reaction method. Effects of calcining time (t) on the crystalline structure, morphology, relative density and shrinkage, the total ionic conductivity of the prepared W, Y, Al-LLZO solid electrolyte were studied, respectively. Controlling suitable calcining time can stabilize cubic phase W, Y, Al-LLZO at room temperature and improve the relative density and the ionic conductivity of the solid electrolyte samples. The relative density and the room temperature ionic conductivity of the W, Y, Al-LLZO solid electrolyte calcined at 900 °C for 6 h are 90.78 % and $2.31 \times 10^{-4} \text{ S}\cdot\text{cm}^{-1}$ respectively.

1. Introduction

Due to potential safety risks such as volatilization, flammability and explosion of organic liquid electrolytes used in lithium-ion batteries, the demand for higher safety electrolytes is increasing [1, 2]. The safety of inorganic solid electrolytes exceeds significantly that of organic liquid electrolytes. Garnet-type $\text{Li}_7\text{La}_3\text{Zr}_2\text{O}_{12}$ (LLZO) is considered to be the next generation of electrolytes, due to its high conductivity and good thermal stability [3, 4]. The ion conductivity of the cubic phase LLZO has much higher than that of the tetragonal phase LLZO. Element doping effectively stabilized the cubic LLZO [5-8]. Our research found that the co-doping of W, Y and Al in LLZO improved significantly the room temperature ionic conductivity of LLZO [9].

In this paper, the W, Y and Al co-doped LLZO were prepared using the solid-state reaction method. Effects of calcining time (t) on the crystalline structure, morphology, relative density and shrinkage, the total ionic conductivity of the solid electrolyte were investigated by X-ray diffraction (XRD), scanning electron microscopy (SEM) and electrochemical impedance spectroscopy (EIS) techniques, respectively.

2. Experimental

2.1 Preparation of the solid electrolyte sample

Samples of $\text{Li}_{5.76}\text{La}_3\text{Zr}_{1.59}\text{W}_{0.35}\text{Y}_{0.06}\text{Al}_{0.2}\text{O}_{12}$ (W, Y, Al-LLZO) were prepared using solid-state reaction method according to the literature [9]. Stoichiometric amounts of Li_2CO_3 [analytical reagent grade



(AR)], La_2O_3 (99.999 %), ZrO_2 (AR), WO_3 (AR), Y_2O_3 (99.999 %), Al_2O_3 (99.999 %) were mixed and ball-milled using a QM-BP planetary ball mill with isopropyl alcohol as the dispersing reagent in agate jar for 12 h, 10 % excess of Li_2CO_3 was added to make up for the loss of lithium compounds in the following high heating stage. The mixed powder was dried in the oven at $105\text{ }^\circ\text{C}$ for 2 h. The dried powder was calcined at $900\text{ }^\circ\text{C}$ for 3, 6, 9, 12, and 15 h respectively. After mixture, drying and calcining at the same condition once more, the calcined powders were pressed into pellet with a diameter of 13 mm with 20MPa pressure. The pellet was covered with self-source powder and sintered at $1160\text{ }^\circ\text{C}$ for 10 h in air. The solid electrolyte sample was obtained.

2.2 Physical characterization

The crystalline structures of the prepared solid electrolyte samples were determined by a diffractometer (Bruker AXS D8 Advance) with Cu K α radiation and $2\theta = 10^\circ \sim 60^\circ$.

The morphologies of the cross-section of the prepared solid electrolyte samples were characterized with scanning electron microcopy (HITACHI S3400N).

The relative density of the prepared solid electrolyte samples was measured by the Archimedes method. The relative shrinkage is calculated with the diameter of pressed pellet and sintered pellet.

The ionic conductivity of the prepared solid electrolyte samples was determined using a solartron impedance analyzer (Solartron 1260 & 1287) with $100\text{Hz} \sim 10\text{MHz}$ frequency range and 10 mV amplitude.

3. Results and discussion

3.1 XRD studies

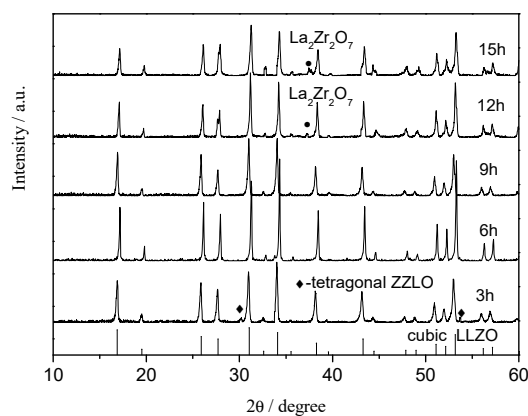


Figure 1. XRD spectra of the W, Y, Al-LLZO solid electrolyte samples for different t . XRD spectra of the W, Y, Al-LLZO solid electrolyte samples for different t are shown in Figure 1. The peaks are labeled with the cubic phase LLZO (ICSD 422259, the vertical lines in the bottom). As shown in Figure 1, when $t = 3$ h, in addition to the peaks of the cubic phase LLZO, the diffraction peak at $2\theta = 30.5^\circ$ change to 2 peaks, number of the diffraction peaks in $50^\circ \leq 2\theta \leq 55^\circ$ are four, which indicate the existence of the tetragonal phase in the solid electrolyte samples [10]. When $t = 6$ or 9 h, the diffraction peaks can match well with the diffraction peaks of the cubic LLZO, which indicates that the solid electrolyte samples are the cubic phase. When $t = 12$ or 15 h, in addition to the peaks of the cubic phase LLZO, the diffraction peak of $\text{La}_2\text{Zr}_2\text{O}_7$ is appeared, which indicate the existence of $\text{La}_2\text{Zr}_2\text{O}_7$ impurity in the solid electrolyte samples.

3.2 SEM images

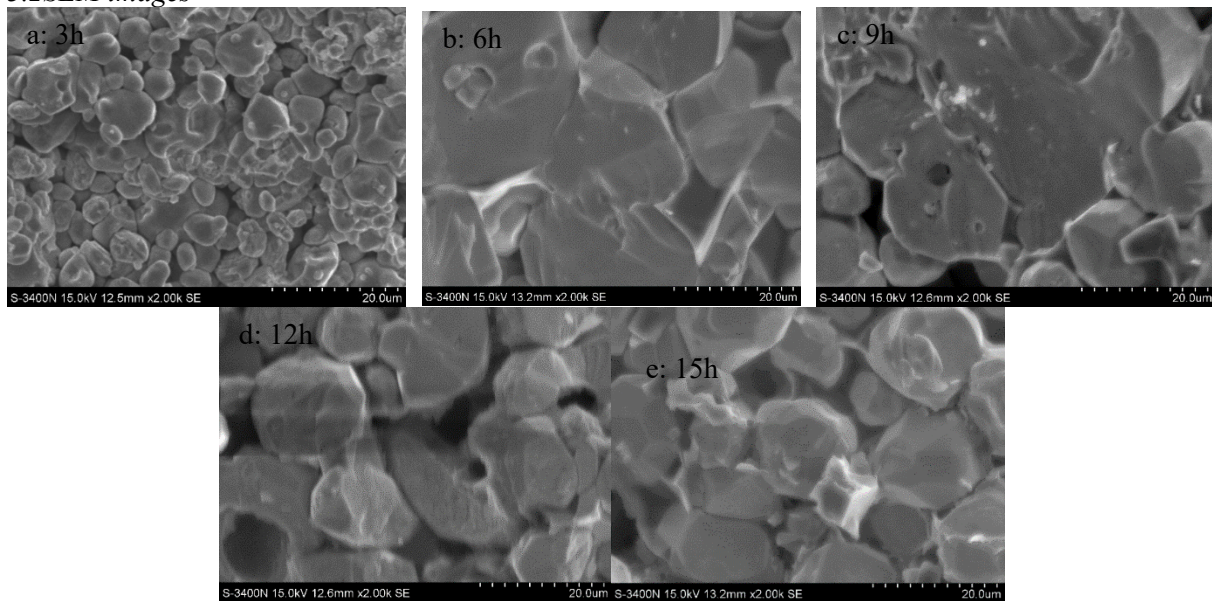


Figure 2. SEM images of the cross-section of the W, Y, Al-LLZO solid electrolyte samples for different t .

The morphologies of the cross-section of the W, Y, Al-LLZO solid electrolyte samples for different t are shown in Figure 2. As shown in Figure 2, when $t = 3$ h, the grain sizes are in the ranges of $1 \sim 6 \mu\text{m}$, the contact between particles is not close, which means a low density. When $t = 6$ h, the grain sizes become the bigger, and the contact between particles is better, which is beneficial to enhancement of densification. With t being in the range of $6 \sim 15$ h, the grain sizes become the smaller and the contact between particles is worse with t increasing, which is not beneficial to enhancement of densification.

3.3 The relative density and shrinkage

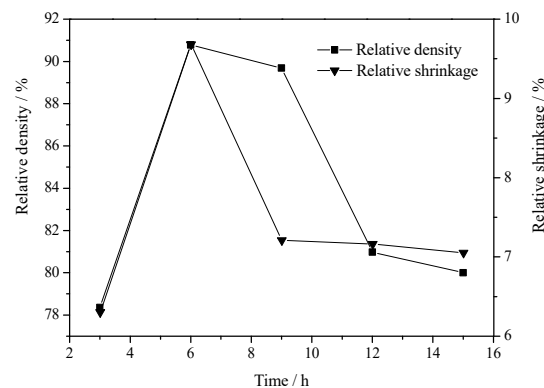


Figure 3. Relative density and shrinkage of the W, Y, Al-LLZO solid electrolyte samples for different t .

The relative density and shrinkage of the W, Y, Al-LLZO solid electrolyte samples for different t are shown in Figure 3. As shown in Figure 3, as t increase, the relative density increases from 78.36 % for $t = 3$ h to 90.78 % for $t = 6$ h. Then, the relative density decreases to 80.00 % for $t = 15$ h. Similarly, for $t = 6$ h, the relative shrinkage is 9.03 %, the value is maximum.

3.4 The ionic conductivity

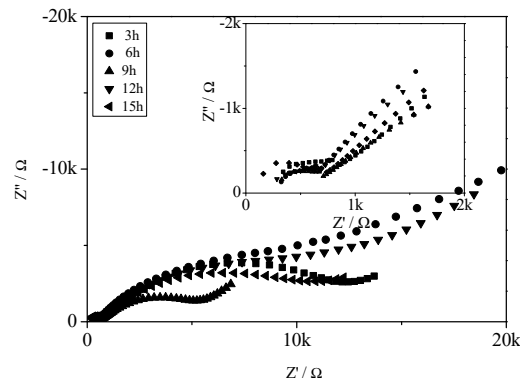


Figure 4. Impedance spectra of the W, Y, Al-LLZO solid electrolyte samples for different t .

Table 1 Conductivity of the W, Y, Al-LLZO solid electrolyte samples for different t

t / h	3	6	9	12	15
$\sigma / S \cdot cm^{-1}$	8.66×10^{-6}	2.15×10^{-4}	2.05×10^{-5}	1.41×10^{-5}	1.17×10^{-5}

The impedance spectra of the W, Y, Al-LLZO solid electrolyte samples for different t measured at 25 °C in air are shown in Figure 4. As shown in Figure 4, a single semicircle and a remarkable diffusion tail are observed in the high frequency region and the low frequency region respectively in the plots of all the samples. The total ionic conductivities (σ) were gotten using ZsimpWin software for simulation to analyzing the impedance data. Table 1 show the total ionic conductivity values of the solid electrolyte samples. From Table 1, the σ increase significantly from $8.66 \times 10^{-6} S \cdot cm^{-1}$ for $t = 3 h$ to $2.15 \times 10^{-4} S \cdot cm^{-1}$ for $t = 6 h$. The relative density increases significantly with t increasing in the range of 3 ~ 6 h, thus the ionic conductivity increases significantly. When t is in the range of 6 ~ 15 h, the σ decreases from $2.15 \times 10^{-4} S \cdot cm^{-1}$ to $1.17 \times 10^{-5} S \cdot cm^{-1}$. The results indicate that controlling t can control the ionic conductivity of the solid electrolyte samples.

4. Conclusions

Controlling suitable calcining time can stabilize cubic phase W, Y, Al-LLZO at room temperature and improve the relative density and the ionic conductivity of the solid electrolyte samples. The relative density and the room temperature ionic conductivity of W, Y, Al-LLZO solid electrolyte calcined at 900 °C for 6 h are 90.78 % and $2.31 \times 10^{-4} S \cdot cm^{-1}$ respectively.

Acknowledgements

This work was financially supported by the Program for National Natural Science Foundation of China (51572176), Shanghai Municipal Education Commission (Plateau Discipline Construction Program, 0817), Collaborative Innovation Fund of Shanghai Institute of Technology (XTCX2017-5).

References

- [1] Koshikawa H., Matsuda S., Kamiya K., Miyayama M., Nakanishi S. (2018) Dynamic changes in charge-transfer resistance at Li metal / $Li_7La_3Zr_2O_{12}$ interfaces during electrochemical Li dissolution / deposition cycles. *Journal of Power Sources*, 376: 147-151.
- [2] Yang T.T., Li Y., Wu W.W., Cao Z.Z., He W.Y., Gao Y.F., Liu J.R., Li G.R. (2018) The synergistic effect of dual substitution of Al and Sb on structure and ionic conductivity of $Li_7La_3Zr_2O_{12}$ ceramic. *Ceramics International*, 44: 1538-1544.
- [3] Nonemacher J.F., Huter C., Zheng H., Malzbender J., Finsterbusch M. (2018) Microstructure and properties investigation of garnet structured $Li_7La_3Zr_2O_{12}$ as electrolyte for all-solid-state batteries.

Solid State Ionics, 321: 126-134.

- [4] Chen X.L., Wang T., Lu W.Z., Cao T.X., Zhang C.M. (2018) Synthesis of Ta and Ca doped $\text{Li}_7\text{La}_3\text{Zr}_2\text{O}_{12}$ solid-state electrolyte via simple solution method and its application in suppressing shuttle effect of Li-S battery. *Journal of Alloys and Compounds*, 744: 386-394.
- [5] Yang X.F., Han X.G., Chen Z.P., Zhou L.H., Jiao W.Z. (2018) Improving the Li-ion conductivity and air stability of cubic $\text{Li}_7\text{La}_3\text{Zr}_2\text{O}_{12}$ by the co-doping of Nb, Y on the Zr site. *Journal of the European Ceramic Society*, 38: 1673-1678.
- [6] Kotobuki M., Song S.F., Takahashi R. (2017) Improvement of Li ion conductivity of $\text{Li}_5\text{La}_3\text{Ta}_2\text{O}_{12}$ solid electrolyte by substitution of Ge for Ta. *Journal of Power Sources*, 349: 105-110.
- [7] Huang M., Xu W., Shen Y., Lin Y.H., Nan C.W. (2013) X ray absorption near-edge spectroscopy study on Ge-doped $\text{Li}_7\text{La}_3\text{Zr}_2\text{O}_{12}$: enhanced ionic conductivity and defect chemistry. *Electrochim. Acta*, 115: 581-586.
- [8] Li Y., Wang Z., Cao Y., Du F., Chen C., Cui Z., Guo X. (2015) W-doped $\text{Li}_7\text{La}_3\text{Zr}_2\text{O}_{12}$ ceramic electrolytes for solid state li-ion batteries. *Electrochim. Acta*, 180: 37-42.
- [9] Liu X.Z., Chen J. (2018) Preparation and application of the LiBaLaZrWREAlO solid electrolyte, C.N. Patent (in Chin.), ZL 201610607959.0, 2018-9-14.
- [10] Rangasamy E., Wolfenstine J., Allen J. (2013) The effect of 24c-site (A) cation substitution on the tetragonal-cubic phase transition in $\text{Li}_{7-x}\text{La}_{3-x}\text{A}_x\text{Zr}_2\text{O}_{12}$ garnet-based ceramic electrolyte. *Journal of Power Sources*, 230: 261-266.